The helix approach

Using dynamic individual pitch control to enhance wake mixing in wind farms

Frederik, Joeri A.; Doekemeijer, Bart M.; Mulders, Sebastiaan P.; van Wingerden, Jan Willem

DOI
10.1002/we.2513

Publication date
2020

Document Version
Final published version

Published in
Wind Energy

Citation (APA)
Frederik, J. A., Doekemeijer, B. M., Mulders, S. P., & van Wingerden, J. W. (2020). The helix approach: Using dynamic individual pitch control to enhance wake mixing in wind farms. *Wind Energy*, *23*(8), 1739-1751. https://doi.org/10.1002/we.2513

Received: 13 December 2019 | Revised: 17 March 2020 | Accepted: 29 March 2020
DOI: 10.1002/we.2513

WILEY

RESEARCH ARTICLE

The helix approach: Using dynamic individual pitch control to enhance wake mixing in wind farms

Joeri A. Frederik | Bart M. Doekemeijer | Sebastiaan P. Mulders | Jan-Willem van Wingerden

Delft Center of Systems and Control, Delft, The Netherlands

Correspondence
Joeri A. Frederik, Delft Center of Systems and Control, TU Delft, Delft 2628 CD, The Netherlands.
Email: j.a.frederik@tudelft.nl

Abstract

Wind farm control using dynamic concepts is a research topic that is receiving an increasing amount of interest. The main concept of this approach is that dynamic variations of the wind turbine control settings lead to higher wake turbulence, and subsequently faster wake recovery due to increased mixing. As a result, downstream turbines experience higher wind speeds, thus increasing their energy capture. In dynamic induction control (DIC), the magnitude of the thrust force of an upstream turbine is varied. Although very effective, this approach also leads to increased power and thrust variations, negatively impacting energy quality and fatigue loading. In this paper, a novel approach for the dynamic control of wind turbines in a wind farm is proposed: using individual pitch control, the fixed-frame tilt and yaw moments on the turbine are varied, thus dynamically manipulating the wake. This strategy is named the *helix approach* because the resulting wake has a helical shape. Large eddy simulations of a two-turbine wind farm show that this approach leads to enhanced wake mixing with minimal power and thrust variations.

KEYWORDS

dynamic induction control, enhanced wake mixing, helix approach, individual pitch control, wake recovery, wind farm control

1 | INTRODUCTION

The interaction between wind turbines in a wind farm through their wakes is a phenomenon that has been studied for decades[1-3] and is still a relevant topic today.[4,5] For the purpose of power maximization, load minimization, or power reference tracking, this interaction can be manipulated using techniques from the control engineering community. In this paper, the focus will be on wind farm power maximization.

In wind farm control, two different approaches can be distinguished: induction control (sometimes called derating control) and wake redirection control (sometimes called wake steering). The former approach uses the induction factor, that is, the in-wake velocity deficit, of the turbines as control input, whereas the latter approach exploits the yaw angle of turbines. Both approaches follow the same strategy: the upstream machines in a wind turbine array will lose power due to locally suboptimal induction or yaw settings, and downstream machines experience higher wind speeds which increases their power production.

The examples of induction control and wake redirection control are plentiful. Induction control has shown promising results in different simulation environments using model-free optimization[6,7] or model predictive control.[8] However, recent studies with high-fidelity simulation models,[9] scaled wind tunnel experiments,[10] and full-scale experiments[11] indicate that the potential wind farm power gain of induction control is minor to nonexistent. Therefore, the focus in the literature for power maximization in wind farms is shifted towards wake redirection.

Peer Review The peer review history for this article is available at https://publons.com/publon/10.1002/we.2513.
Short title: On the helix approach to enhance wake mixing in wind farms

Wake deflection through yaw is first modeled in Jiménez et al,[12] and extensive research has been executed since. For example, Annoni et al,[4,5] Howland et al,[13] and Vollmer et al[14] study the wake of a yawed turbine,[15,16] conduct simulation studies, and[17] full-scale experiments using lidar measurements. Both scaled wind tunnel experiments[18] and full-scale tests[19,20] indicate that this strategy can effectively increase the power production of a wind farm. Furthermore, Siemens Gamesa has recently launched a commercial wake steering product.[21] A comprehensive survey on wind farm modeling and control can be found in Boersma et al,[22] whereas Kheirabadi and Nagamune[23] gives an overview of research on wind farm power maximization. All these references have in common that they focus on steady-state optimal control of a wind farm. Therefore, time-varying control inputs that purposely influence the inherently dynamic nature of the wind are disregarded.

To the best of the authors' knowledge, the first mention of dynamic control being used to increase the performance of wind farms is in an industrial patent.[24] This patent describes different control methods involving either dynamic induction, dynamic yawing, or wake deformation through cyclic pitch signals. What these control methods have in common is that they aim to increase wake mixing by changing the control inputs over time. Wake mixing is the phenomenon where the wake interacts with the adjacent, higher velocity, and free-stream flow. As a result, the wake recovers some of the energy extracted by the upstream turbine, such that a downstream turbine experiences a higher wind velocity. However, only the general idea is described; no experiments or simulations are performed, and the effectiveness of these methods is not evaluated.

Recently, dynamic wind farm control has gained interest in the scientific field, initiated by the work presented in Goit and Meyers.[25] Dynamic induction control (DIC) specifically is a research topic that has seen a number of publications studying its potential in simulations[26-28] and in scaled wind tunnel experiments.[29] To enable practical implementation, the most recent papers focus on a smaller subset of dynamic signals, namely, sinusoidal signals.[28] In Munters and Meyers,[28] a grid search is performed using large eddy simulations (LESs) to determine the amplitude and frequency of the sinusoidal excitation that maximize the farm-wide power production. In Frederik et al,[29] wind tunnel experiments are performed to validate this approach, showing positive results. A different dynamic control approach is investigated using high-fidelity simulations in Munters and Meyers[30] and Kimura et al.[31] Here, the yaw angle of a turbine is varied dynamically, such that increased wake meandering is induced.

The above-mentioned approaches do have an important drawback: because of the varying induction factor or yaw angle signals of the upstream turbine, the thrust force on the rotor varies significantly. As a result, this turbine experiences substantial power and load fluctuations, which is disadvantageous from a power quality perspective. In this paper, a novel approach to dynamic wake mixing is introduced, which is expected to lead to lower power and thrust variations. This approach makes use of individual pitch control (IPC), a procedure in which the blade pitch angles of a wind turbine are controlled independently of each other.

IPC is a well-known strategy in the wind turbine control community. It is usually applied to alleviate periodic loads on turbines with minimal power loss, as first proposed proposed by Bossanyi.[32,33] Further research into load reducing IPC algorithms is still a relevant research direction, for example, into using an azimuth offset[34] or implementing more advanced control strategies.[35-37] Research where IPC is used to increase the power production of a wind farm is limited. Experiments have been conducted where IPC is used for wake steering[38] or power maximization in case of partial wake overlap.[15] However, the results were inconclusive, and no further research has been published since.

In this paper, wake steering through individual pitch control is combined with the concept of dynamic wind farm control to forge a novel approach. This approach, called dynamic IPC (DIPC), uses the multi-blade coordinate (MBC) transformations to vary the tilt and yaw moments on the rotor. Thus, the wake is manipulated, slowly varying its direction over time. This is hypothesized to result in enhanced wake mixing, such that downstream turbines in a wind turbine array can increase their power production with minimal rotor thrust fluctuations. A patent by the authors describing this concept is pending.[39]

The main contributions of this paper are threefold. First of all, the novel DIPC approach is described. Second, a specific DIPC strategy called the *helix approach* is defined, which dynamically moves the wake both horizontally and vertically. Finally, the effectiveness of this helix approach is evaluated through high-fidelity simulations. These simulations are executed using the LES code Simulator fOr Wind Farm Applications (SOWFAs).[40] The effects of DIPC both on the wake and on a downstream turbine are investigated. A thorough comparison is made with existing control strategies to evaluate the performance of DIPC.

This paper is organized as follows: in Section 2, the simulation environment is defined. Section 3 thoroughly describes the working principles of DIPC in general and the helix approach specifically. The potential of this approach as a wind farm control approach will then be demonstrated in Section 4 through high-fidelity simulations. Finally, conclusions are drawn, and future work is discussed in Section 5.

2 | SIMULATION ENVIRONMENT

The proposed control strategy is evaluated in SOWFA,[40] which is a high-fidelity simulation environment developed by the US National Renewable Energy Laboratory (NREL). SOWFA is a large-eddy solver for the fluid dynamics in the turbulent atmosphere. The interaction with one or multiple wind turbines[41] is included in SOWFA. Turbines are modeled as actuator disks or actuator lines as demonstrated in Sorensen and Shen.[42] The SOWFA source code was adapted to allow for specifications of a different pitch setpoint for each individual blade, enabling the implementation of IPC.

In this work, two different simulation cases are defined. First of all, wind with a uniform inflow profile is used to demonstrate the working principles of DIPC. It is recognized that these conditions do not represent realistic working conditions in an actual wind farm. However, due to the absence of turbulence, these simulations are perfectly suited to visualize the effects of DIPC on the wake of a turbine, as presented in Section 3.

Variable	Case I: uniform flow	Case II: turbulent flow
Turbine	DTU 10 MW[43]	DTU 10 MW[43]
Rotor diameter	178.3 m	178.3 m
Domain size	2.5 km ×1 km × 0.6 km	3 km ×3 km × 1 km
Cell size (outer region)	50 m ×50 m × 50 m	10 m ×10 m × 10 m
Cell size (near rotor)	3.125 m ×3.125 m × 3.125 m	1.25 m ×1.25 m × 1.25 m
ABL stability	Neutral	Neutral
Inflow hub height wind speed	9.0 m/s	9.0 m/s
Inflow turbulence intensity	0.0%	5.0%
Surface roughness	0.0 m	$2.0 \cdot 10^{-4}$ m

TABLE 1 Numerical simulation scheme in simulator for wind farm application (SOWFA) for uniform simulations

Abbreviation: ABL, atmospheric boundary layer; DTU, Danmarks Tekniske Universitet.

The second simulation case employs more realistic wind conditions to evaluate the potential of DIPC. These simulations are of a neutral atmospheric boundary layer (ABL) in which the inflow was generated through a so-called precursor simulation. Several properties of both simulation setups are listed in Table 1.

Two different wind farm cases are investigated in these conditions. First, simulations with a single turbine, in which the effects on the turbine and wake are investigated, have been executed. Then, a second turbine is added, to assess the gain in energy capture that can be achieved with DIPC. The second turbine is situated five rotor diameters (5*D*) behind the upstream turbine, the same axial distance as investigated in Frederik et al.[29] All these results are presented in Section 4.

3 | CONTROL STRATEGY

In this section, the DIPC strategy is further elaborated, as well as the already existing control strategies with which it will be compared. In Section 3.1, static induction strategies are explained, which includes *greedy* control, where each turbine operates using its individual steady-state optimal settings. These strategies are currently the industry standard and commonly applied in actual wind farms. They therefore serve as a useful baseline case for cutting edge control concepts such as periodic DIC and the novel DIPC approach. Periodic DIC, as described in Frederik et al,[29] is shortly covered in Section 3.2, and Section 3.3 presents a thorough explanation of the DIPC approach as proposed in this paper.

3.1 | Static induction control

Static induction control (SIC) is a generic term for all induction control strategies that use time-invariant control set-points that depend on the inflow conditions. The most simple static induction wind farm control strategy is to operate all turbines at their individual (static) optimum for power production. This approach is called *greedy control*, as all turbines greedily extract as much power from the wind as possible. As this approach is the simplest and most commonly applied, greedy control is considered the baseline case in this paper.

An alternative approach is to (statically) lower the induction factor, that is, the in-wake velocity deficit, of upstream turbines such that downstream turbines can increase their power capture. This has for long been the most popular concept in wind farm control research, but recent studies show that the achievable gains with respect to greedy control are minor to nonexistent.[9,10,44] Nonetheless, SIC for power maximization remains of interest to the industry. Hence, it is used as a comparison case in this article to show the potential of DIPC.

3.2 | Periodic DIC

A recent research area of interest, as an alternative to SIC, is DIC. With this control method, the induction factor of an upstream turbine is varied over time to enhance wake mixing, such that downstream turbines experience higher wind velocities and can subsequently increase their power production. Finding the optimal time-varying induction settings is a very complex control problem.[27] A more practical approach is proposed in Munters and Meyers,[28] where sinusoidal input signals on the thrust force C_T' are suggested. This method is called periodic DIC and will also be used in this paper. It is shown to increase the power production of small wind farms both in simulations[28] and in wind tunnel experiments.[29]

In Frederik et al,[29] for reasons of practical implementation, a periodic excitation is realized by superimposing a low-frequent sinusoidal signal on the static collective pitch angles of the turbine. This approach will also be used in this paper. As the control signal is now confined to a sinusoid, the control parameters are reduced to the amplitude and the frequency of excitation. The frequency is usually characterized in terms of the dimensionless Strouhal number *St*:

$$St = \frac{f_e D}{U_\infty}, \tag{1}$$

where f_e is the frequency [Hz], D the rotor diameter [m], and U_∞ the inflow velocity [m/s]. As the Strouhal number is dimensionless, it accounts for different turbine sizes or inflow velocities. In the above-mentioned references, an optimal Strouhal number of $St \approx 0.25$ is found experimentally. For the DTU 10MW turbine,[43] with an inflow velocity of 9 m/s, an excitation frequency of $f_e = 0.0126$ Hz is found. To verify this optimal frequency, an extensive evaluation is performed in SOWFA. A single 10-MW wind turbine is placed in laminar flow conditions (see Table 1), and the velocity is measured at integer multiples of the rotor diameters D behind the turbine. The results are presented in Figure 1 and show that

for a distance $\geq 5D$, the optimum is indeed around $St = 0.25$. As a physical explanation for the optimal frequency is not yet investigated, this excitation frequency was used in the simulations presented here. To take into account the effect of different excitation amplitudes, two different DIC cases will be considered: a low amplitude case with a collective pitch amplitude of 2.5° and a high amplitude case of 4°, respectively.

3.3 | Dynamic individual pitch control

In this section, the novel DIPC approach will be described. The goal of this approach is to enhance wake mixing analogous to DIC, but without the large fluctuations in thrust and power. To achieve this, the individual pitch angles are altered in such a way that the wake behind the excited turbine is manipulated dynamically.

Fundamentally, DIPC works as follows. The individual blade pitch angles of the turbine can be used to generate a directional moment on the rotor. Consequently, the direction of the force vector exerted on the airflow can be manipulated. With DIPC, the direction of this force vector is slowly varied, thereby continuously changing the direction of the wake. This is expected to increase wake mixing without significant variations in the magnitude of the rotor thrust force.

A directional thrust force can be accomplished by implementing the MBC transformation.[45] This transformation decouples—or stated differently: *projects*—the blade loads in a nonrotating reference frame. As a result, the measured out-of-plane blade root bending moments $M(t) \in \mathbb{R}^3$ are projected onto a nonrotating reference frame. For a three-bladed turbine, the MBC transformation is given as follows:

$$\begin{bmatrix} M_0(t) \\ M_{\text{tilt}}(t) \\ M_{\text{yaw}}(t) \end{bmatrix} = \mathbf{T}(\psi) \underbrace{\begin{bmatrix} M_1(t) \\ M_2(t) \\ M_3(t) \end{bmatrix}}_{M(t)}, \tag{2}$$

with

$$\mathbf{T}(\psi) = \frac{2}{3} \begin{bmatrix} 0.5 & 0.5 & 0.5 \\ \cos(\psi_1) & \cos(\psi_2) & \cos(\psi_3) \\ \sin(\psi_1) & \sin(\psi_2) & \sin(\psi_3) \end{bmatrix},$$

where ψ_b is the azimuth angle for blade b, with $\psi = 0°$ indicating the vertical upright position. The collective mode M_0 represents the cumulative out-of-plane rotor moment, and M_{tilt} and M_{yaw} represent the fixed-frame and azimuth-independent tilt- and yaw-moments, respectively.

In a similar fashion, the inverse MBC transformation can be used to obtain implementable pitch angles based on the fixed-frame collective, tilt, and yaw pitch signals, θ_0, θ_{tilt}, and θ_{yaw}, respectively:

$$\underbrace{\begin{bmatrix} \theta_1(t) \\ \theta_2(t) \\ \theta_3(t) \end{bmatrix}}_{\theta(t)} = \mathbf{T}^{-1}(\psi) \begin{bmatrix} \theta_0(t) \\ \theta_{\text{tilt}}(t) \\ \theta_{\text{yaw}}(t) \end{bmatrix}, \tag{3}$$

with

$$\mathbf{T}^{-1}(\psi) = \begin{bmatrix} 1 & \cos(\psi_1) & \sin(\psi_1) \\ 1 & \cos(\psi_2) & \sin(\psi_2) \\ 1 & \cos(\psi_3) & \sin(\psi_3) \end{bmatrix}.$$

The concept of DIPC is to achieve a dynamically varying tilt and/or yaw moment, such that the wake of the turbine is manipulated in vertical and/or horizontal direction, respectively, over time. To give a proof of concept, a simple feedforward strategy is implemented, where a sinusoidal excitation is superimposed on θ_{tilt} and θ_{yaw}, as shown in Figure 2. The excitation frequency of θ_{tilt} and θ_{yaw} is chosen to be identical to the DIC case, that is, $St = 0.25$. Note once more that this is a low-frequent excitation, typically in the range of 10 times slower than the rotational frequency f_r. It will be shown later that the resulting tilt and yaw moments are indeed sinusoidal with frequency f_e.

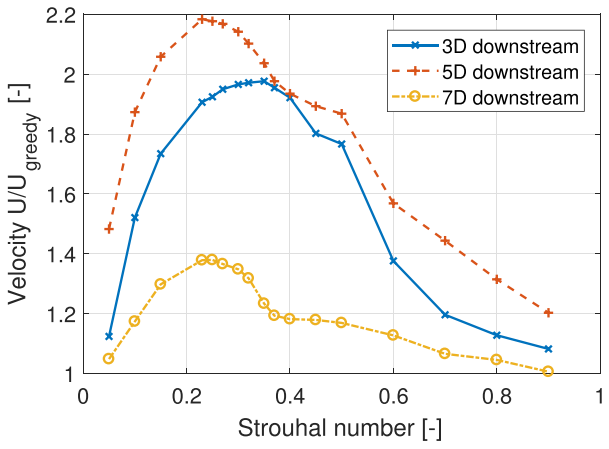

FIGURE 1 The average wake velocity over a hypothetical rotor disk at 3*D*, 5*D*, and 7*D* behind a dynamic induction control (DIC)-excited turbine. DIC was implemented with a pitch amplitude of 4°, for different Strouhal numbers *St*. The results are normalized with respect to the baseline case [Colour figure can be viewed at wileyonlinelibrary.com]

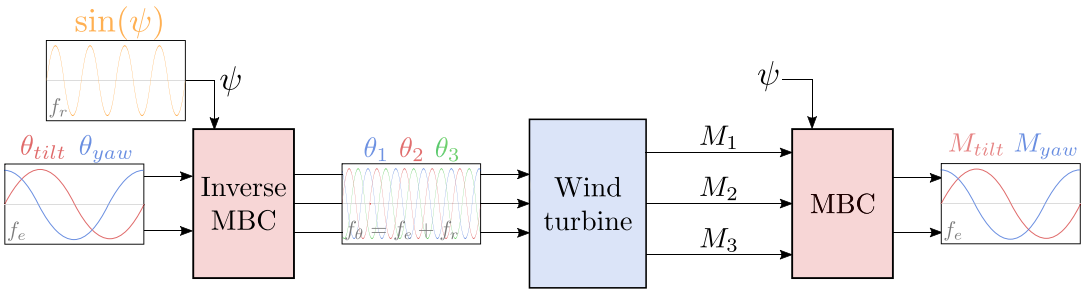

FIGURE 2 A schematic representation of how the MBC transformation is used to achieve periodic yaw and tilt moments on the turbine. The (inverse) MBC transformations are applied to obtain the desired input and output signals. Note that the pitch frequency f_θ is slightly different than the rotation frequency f_r due to excitation frequency f_e. MBC, multi-blade coordinate [Colour figure can be viewed at wileyonlinelibrary.com]

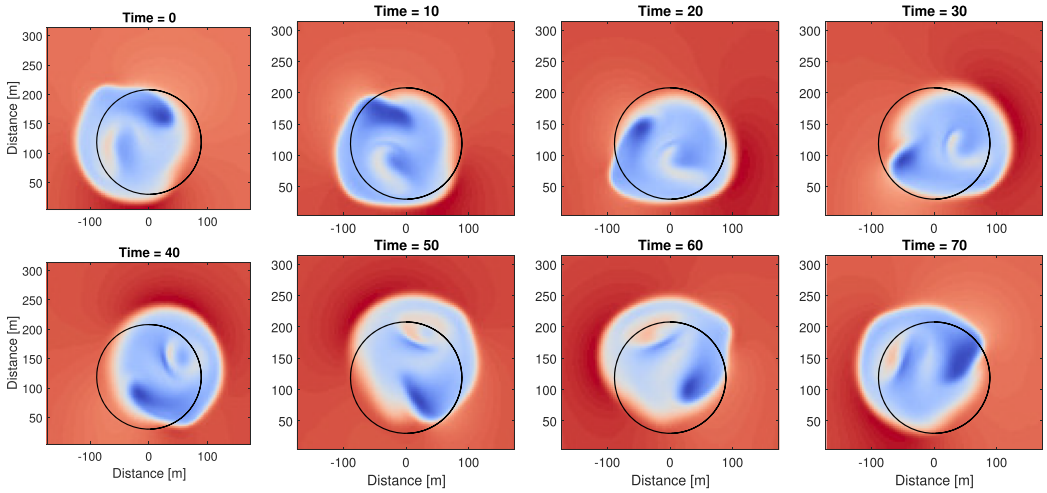

FIGURE 3 A wake at 3*D* behind the turbine, as seen from the front, at different time instances when the signals for θ_{tilt} and θ_{yaw} that create a counterclockwise (CCW) helix are applied. Red areas indicate high wind velocity, that is, undisturbed by the turbine, whereas the blue area indicates a velocity deficit due to the turbine. Clearly, the wake makes a counterclockwise rotation as time progresses. Obtained using uniform inflow simulations in SOWFA [Colour figure can be viewed at wileyonlinelibrary.com]

When the tilt and yaw pitch angles inserted into the inverse MBC transformation are constant over time, the resulting pitch angles $\theta(t)$ will behave sinusoidally with frequency f_r. However, when $\theta_0 = 0$ and the tilt and yaw pitch angles are sinusoidal (with frequency f_e), as depicted in Figures 2, this leads to a slightly altered frequency of $\theta(t)$. Using Equation (3), it can be deduced that

$$\begin{aligned}\theta_b(t) &= \begin{bmatrix} 1 & \cos(\psi_b) & \sin(\psi_b) \end{bmatrix} \begin{bmatrix} \theta_0(t) \\ \theta_{\text{tilt}}(t) \\ \theta_{\text{yaw}}(t) \end{bmatrix} \\ &= \theta_0 + \cos(\omega_r t + \psi_{0,b})\theta_{\text{tilt}}(t) + \sin(\omega_r t + \psi_{0,b})\theta_{\text{yaw}}(t) \\ &= \cos(\omega_r t + \psi_{0,b})\sin(\omega_e t) + \sin(\omega_r t + \psi_{0,b})\cos(\omega_e t) \\ &= \sin\left[(\omega_r + \omega_e)t + \psi_{0,b}\right],\end{aligned}$$

where ω_r is the rotational velocity [rad/s] and $\omega_e = 2\pi f_e$ [rad/s]. Assuming that ω_r is constant over time, $\psi_b(t) = \omega_r t + \psi_{0,b}$ with $\psi_{0,b}$ the azimuth angle of blade b at $t = 0$. Because the excitation frequency is very low (i.e., $\omega_e \ll \omega_r$) the frequency of the resulting sinusoid, f_θ, differs only slightly from the rotational frequency f_r.

In Figure 2, a shift of 90° between the yaw moment and the tilt moment is depicted. As a result, the tilt moment is maximal when the yaw moment is zero, and vice versa. Using the uniform simulation setup in SOWFA, the resulting wake location over time can be visualized. Figure 3 shows this wake at eight instances during one excitation period $T_e = D/(StU_\infty) \approx 80$ s. It can be observed here that this DIPC strategy results in a wake that makes a counterclockwise (CCW) circular motion. This motion can be considered forced wake meandering and is expected to lead to increased wake mixing.

Figure 3 displays the wake for a phase delay of 90° between the tilt and yaw pitch angle, leading to a CCW motion of this wake as seen from upstream. It is also possible to force the wake into a clockwise (CW) motion by applying a phase delay of 270°. In that case, the resulting pitch

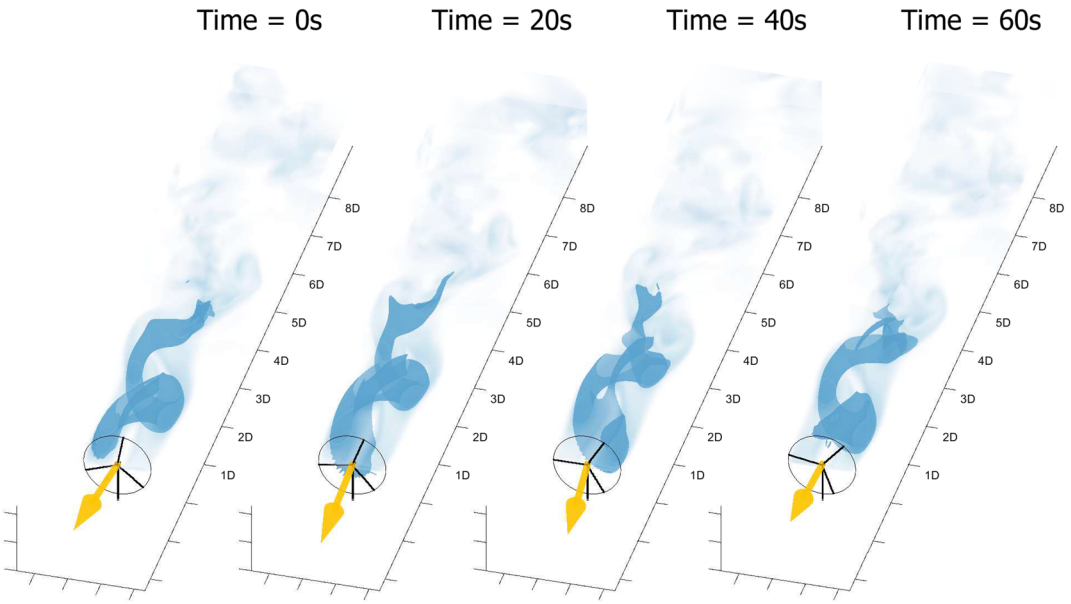

FIGURE 4 An illustrative visualization of the wake propagation for different time instances when the helix strategy is applied. The darker blue shading are iso-surfaces for a velocity in the x-direction of 4 m/s. On the $x-y$-plane, the absolute wind velocity is plotted in lighter blue. The counterclockwise rotation of the wake can be seen, and the near wake clearly exhibits the helix shape that the approach is named after. The yellow arrow represents the vector of the thrust applied on the flow. Obtained using uniform inflow simulations in SOWFA with a free-stream velocity of 9 m/s [Colour figure can be viewed at wileyonlinelibrary.com]

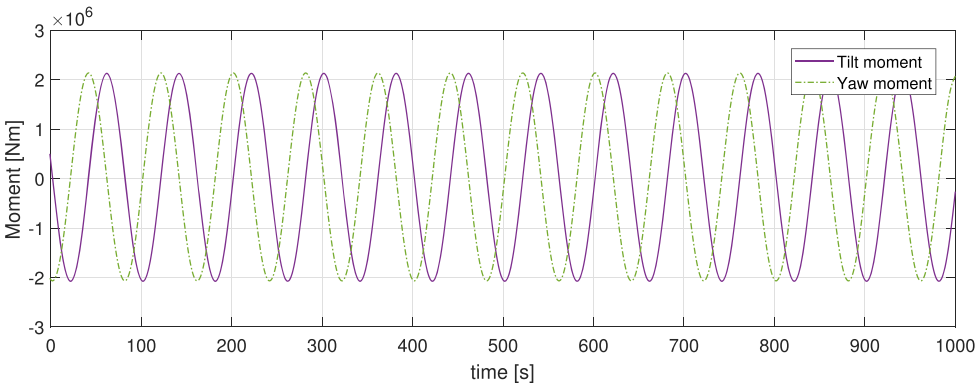

FIGURE 5 The tilt and yaw moments from a turbine operating with the counterclockwise (CCW) helix approach. As can be seen, implementing tilt and yaw angles and applying the inverse multi-blade coordinate (MBC) transformation is an effective method to obtain the desired sinusoidal tilt and yaw moments. Obtained using uniform inflow conditions in SOWFA [Colour figure can be viewed at wileyonlinelibrary.com]

frequency will be slightly *lower* than the rotation frequency:

$$\begin{aligned}\theta_b(t) &= \cos(\omega_b t)\sin(\omega_e t) - \sin(\omega_b t)\cos(\omega_e t)\\ &= -\sin\left[(\omega_b - \omega_e)t\right].\end{aligned}$$

As the resulting wake propagates through space in a helical fashion, this specific approach is called the *helix strategy*, respectively in CCW or CW direction. This helical wake propagation is illustrated in Figure 4.

Earlier in this section, the claim was made that a sinusoidal tilt and yaw moment can be achieved by simply applying a sinusoidal tilt and yaw angle. To confirm that this is indeed the case, Figure 5 shows the tilt and yaw moment for the CCW helix strategy. These moments were obtained using the out-of-plane root bending moments on the individual blades as obtained from SOWFA, subsequently projected onto the nonrotating frame using the MBC transformation (2). Afterwards, a low-pass filter was applied to account for high frequency noise. Note that the amplitude of both signals is identical and that a phase offset of 90° can indeed be observed.

4 | RESULTS

In this section, the results obtained from the SOWFA simulations with turbulent inflow, as described in Section 2, are presented. The helix approach is compared with the baseline greedy control case, as well as with SIC and DIC. First, simulations with a single turbine are evaluated. These simulations allow for the investigation of the helix approach on the excited turbine and on the wake behind this turbine. Afterwards, a

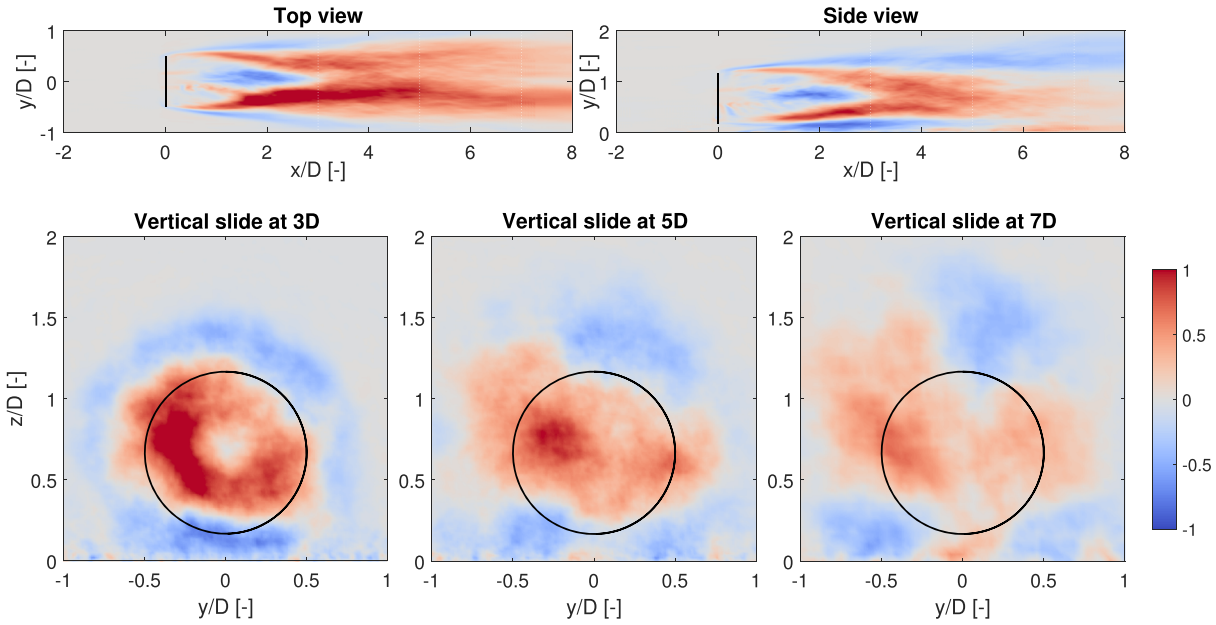

FIGURE 6 The mean magnitude of the wind velocity vector in a wake with respect to the baseline case when dynamic induction control (DIC) is applied (Case 7). The turbine location is indicated in black. The top figures give a top and side view of the flow, and the bottom figures show vertical slices at different distances behind the excited turbine. The red areas indicate that DIC increases the wind velocity in the wake significantly, whereas blue areas indicate where the wind speed is decreased [Colour figure can be viewed at wileyonlinelibrary.com]

second turbine is placed in the wake, 5*D* behind the first turbine, to study the effect of DIPC on this downstream machine and on the power production of this small two-turbine wind farm.

4.1 | Single turbine

For the single turbine case, a total of nine different simulations have been carried out. A comparison between cases will be made based on both the performance of the turbine and the energy available in the wake. The simulation cases are specified below:

1. *Baseline case*: static greedy control. All other cases will be normalized with respect to this case;
2. *SIC*, *1°*: SIC where the collective pitch angles are derated with 1° towards feather;
3. *SIC*, *2°*: Same as Case 2, but with the pitch angles derated 2°;
4. *DIC*, *2.5°*: DIC where the collective pitch angles are excited sinusoidally with an amplitude of 2.5° and a frequency of $St = 0.25$ ($f = 0.0126$ Hz);
5. *CCW helix*, *2.5°*: the helix approach with a phase offset between tilt and yaw moments of 90° (as shown in Figure 2). This results in a wake that rotates in CCW direction. The amplitude of the tilt and yaw angles is chosen such that the variation of the implemented pitch angles has an amplitude of 2.5°;
6. *CW helix*, *2.5°*: the helix approach with a phase offset between tilt and yaw moments of 270°. This results in a wake rotating in CW direction;
7. *DIC*, *4°*: Same as Case 4, but with an amplitude of 4°;
8. *CCW helix*, *4°*: Same as Case 5, but with an amplitude of 4°;
9. *CW helix*, *4°*: Same as Case 6, but with an amplitude of 4°.

First of all, the effect of the helix approach on the wake is investigated. For this purpose, the mean wind velocity behind the excited turbine is visualized with respect to the baseline case. The resulting figures show how the applied control algorithms change the wake properties. Figure 6 shows this mean velocity disparity with respect to the baseline case for Case 7 (DIC, 4°). Different cross-sections of the flow field are depicted here to show the effect of DIC on the average wake velocity. Figure 7 depicts the same cross-sections for the Case 8 (CCW helix, 4°) and Figure 8 for Case 9 (CW helix, 4°). Remember that, as mentioned in Section 3.3, the optimal amplitude and frequency for the helix approach are as of yet unknown. The results presented here should therefore be considered a proof of concept for this approach, not an upper limit of its potential.

Based on these figures, a number of conclusions are drawn. First of all, it is clear that all three strategies successfully increase the average wind velocity in the wake. DIC and CCW helix seem to be equally effective at 3*D*, whereas the helix approach performs increasingly well further downstream. In general, the CW helix appears to be less effective than the CCW helix. Figure 8 reveals that the lower performance of the CW approach is caused by the lower velocity in the center of the wake, which is considerably more distinct than in Figure 7.

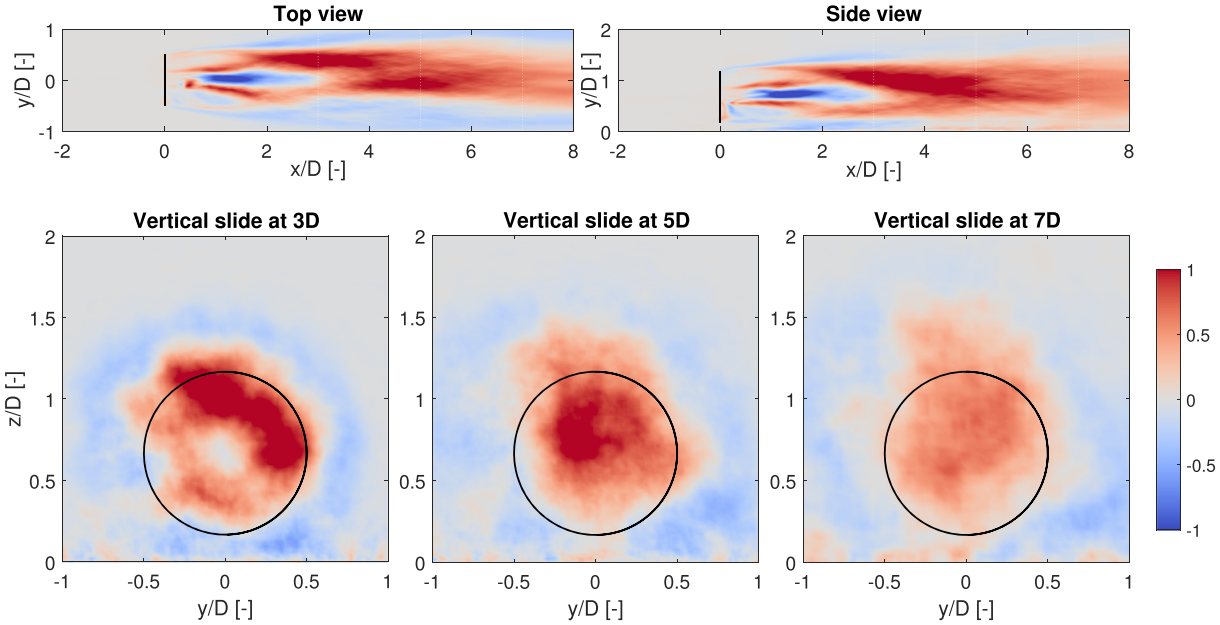

FIGURE 7 The mean magnitude of the wind velocity vector in a wake with respect to the baseline case when counterclockwise (CCW) helix is applied (Case 8). The turbine location is indicated in black. The top figures give a top and side view of the flow, and the bottom figures show vertical slices at different distances behind the excited turbine. The red areas indicate that CCW helix increases the wind velocity in the wake significantly, whereas blue areas indicate where the wind speed is decreased [Colour figure can be viewed at wileyonlinelibrary.com]

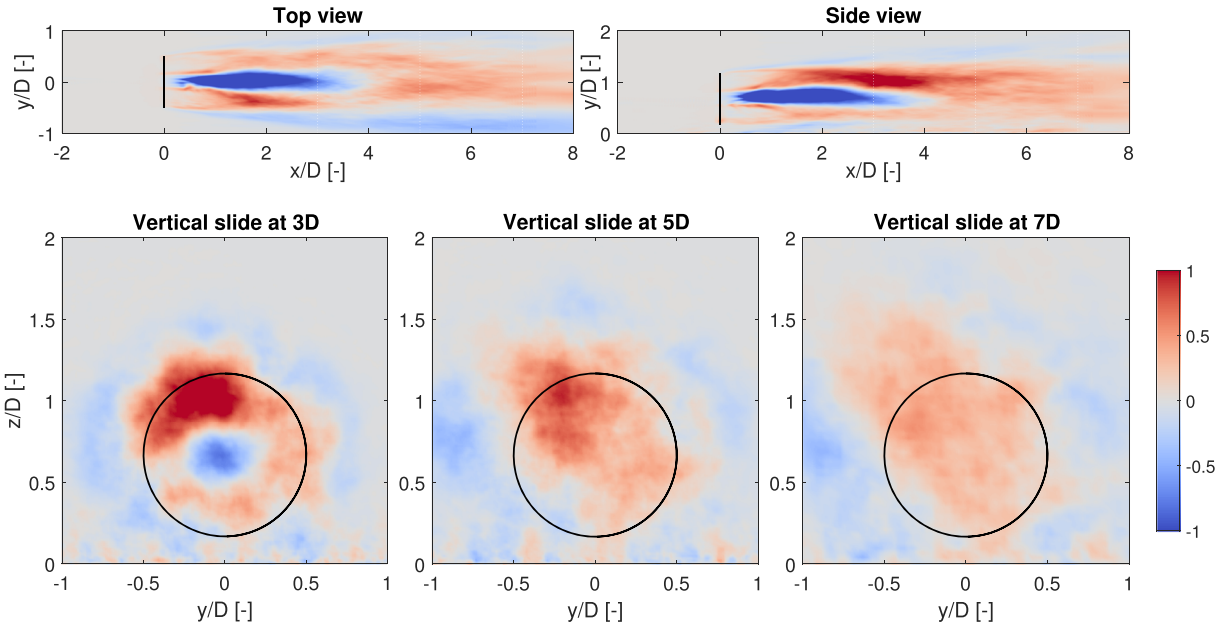

FIGURE 8 The mean magnitude of the wind velocity vector in a wake with respect to the baseline case when clockwise (CW) helix is applied (Case 9). The turbine location is indicated in black. The top figures give a top and side view of the flow, and the bottom figures show vertical slices at different distances behind the excited turbine. The red areas indicate that CW helix increases the wind velocity in the wake significantly, whereas blue areas indicate where the wind speed is decreased [Colour figure can be viewed at wileyonlinelibrary.com]

The average kinetic energy increase in the wake at 5*D* behind the turbine is 23.8% for DIC, 36.7% for CCW helix, and 19.3% for CW helix. This indicates that the power increase that can be expected of a second, waked turbine when the CCW helix is applied will be higher than in the DIC case. As observed in Fleming et al,[15,38] the effect of static IPC wake steering on the wake centerline is limited—much smaller than with wake redirection by yaw or tilt. It can therefore be concluded that the velocity increase in the wake found here is a result of the increased turbulence induced by the dynamic IPC signals. As a result, the interaction of the wake with the free-stream flow is increased, resulting in increased wake recovery.

Note that for both DIC and the helix approach, the wake velocity around the wake is decreased with respect to the baseline case. This is visualized by the blue regions around the hypothetical rotor disk in Figures 6, 7, and 8. Although this phenomenon is yet to be investigated, it

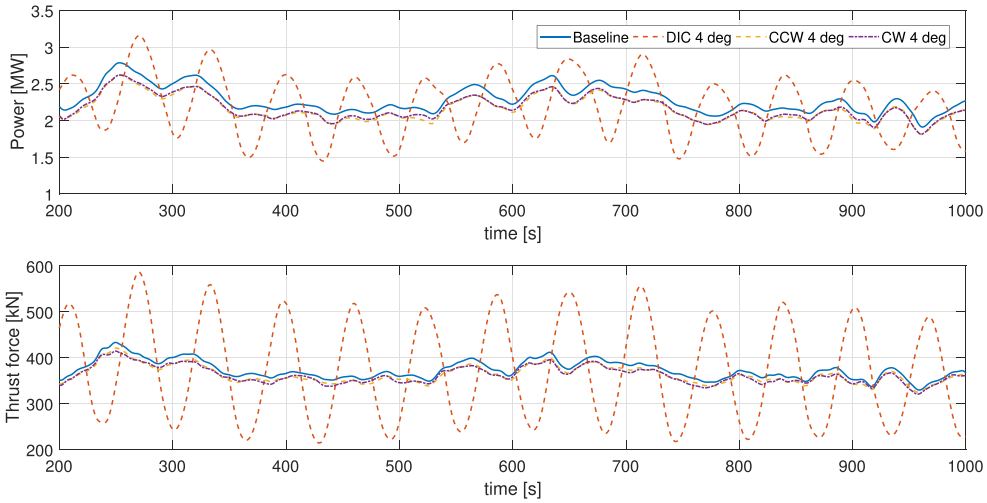

FIGURE 9 The power (top) and thrust (bottom) signals of the wind turbine for the baseline, DIC, CCW helix, and CW helix case. CCW, counterclockwise; CW, clockwise; DIC, dynamic induction control [Colour figure can be viewed at wileyonlinelibrary.com]

TABLE 2 Turbulent inflow, single turbine results

	Static 1°	Static 2°	DIC 2.5°	CCW Helix 2.5°	CW Helix 2.5°	DIC 4°	CCW Helix 4°	CW Helix 4°
Power	-1.0%	-3.1%	-1.1%	-1.1%	-1.0%	-2.8%	-2.8%	-2.6%
Variation of power	-2.2%	-5.8%	+79.5%	-3.5%	-1.5%	+194.1%	-7.9%	-5.2%
Variation of thrust	-11.2%	−22.1%	+583.2%	-1.5%	+1.2%	+1423%	-3.7%	+0.3%
Energy at 3*D*	+14.1%	+31.7%	+20.3%	+20.5%	+7.2%	+42.6%	+47.4%	+21.9%
Energy at 5*D*	+3.7%	+8.3%	+13.3%	+16.6%	+6.5%	+23.8%	+36.7%	+19.3%
Energy at 7*D*	+2.0%	+3.7%	+7.3%	+12.4%	+5.5%	+13.4%	+25.6%	+14.7%
Pitch variation [°/min]	0	0	0.08	4.94	3.22	0.20	12.52	8.13

Note. All but the pitch rate are relative results with respect to the baseline case. Abbreviations: CCW, counterclockwise; CW, clockwise; DIC, dynamic induction control.

suggests that the helix is most effective in the case of full wake overlap. Therefore, the gains reported here hold under the assumption that full wake interaction between turbines consistently takes place.

The mean wake velocities are nonetheless not the most significant difference between DIC and the helix approach. The main advantage of the helix approach becomes clear when the power and thrust signals of the excited turbine are examined, as shown in Figure 9. These plots shows that, as expected, DIC results in large variations of both the power production and the thrust force. Both helix approach simulations show no such variations: the power and thrust are in both cases very similar to the baseline case, although slightly lower. This is also confirmed when the variance of these signals is calculated. When DIC is applied, the variance of the power and the thrust increases—compared with the baseline case—with 80% and 583%, respectively. With the helix approach, on the other hand, the variance of these signals stays more or less the same with respect to the baseline case.

This significant improvement with regards to the thrust and power variations does not come completely free of charge. Because IPC is used for the helix method, the pitch rate, and subsequently the actuator duty cycle, is higher than with DIC. As visualized in Figure 2, the frequency of the pitch signal is determined by the rotational frequency $f_r \approx 0.12$ Hz, slightly altered by the excitation frequency. The pitch signals in DIC, on the other hand, have a much lower frequency of $f_e \approx 0.0126$ Hz, resulting in a very low average pitch variation of 0.08 °/min. As a consequence of the higher pitch frequency, the pitch variance of the helix approach with a 4° amplitude is 12.5 and 8.1°/min for the CCW and CW direction, respectively. Note that although this is significantly higher than with DIC, such a pitch rate should not be considered unreasonably high. In fact, the pitch rate is comparable with that used in load alleviating IPC strategies such as Bossanyi.[32,33] Another potential negative side-effect of (dynamic) IPC mentioned in Bossanyi[32] is that the cyclic pitch actuation might cause increased loadings on essential elements of the turbine, such as the blades, shaft and yaw bearings. These loads are not considered in this paper. Instead, the variation of the turbine thrust force is used as a rough indicator of potential loads on the turbine caused by DIPC.

All the results mentioned above, both in terms of turbine performance and wake recovery, are summarized in Table 2. This table includes the results obtained for the cases with SIC and with a smaller pitch amplitude of 2.5°. As expected, the lower amplitude has less effect on both the excited turbine and the wake recovery. Apart from that, no significant discrepancies are found between the 2.5° and 4° cases. The SIC results show that, in general, the power lost at the upstream turbine is comparable, whereas the energy gained in the wake is lower than with the CCW helix approach. Even more so than DIC, SIC seems to be less effective at larger downstream distances. It can therefore be concluded that the helix approach is more effective in increasing the potential energy capture of a wind farm than SIC.

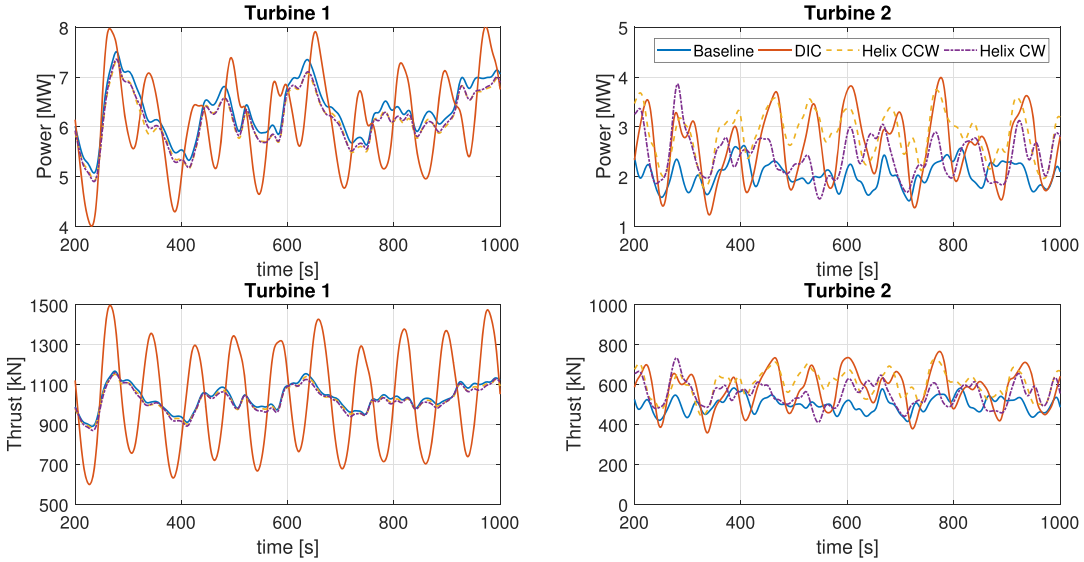

FIGURE 10 The power (top) and thrust (bottom) signals of turbines 1 (left) and 2 (right) for Cases 1, 5, 6, and 7. The variations in power and thrust associated with DIC are not present with the helix approach. As a result, the power and thrust variations at the downstream turbine are also significantly lower. CCW, counterclockwise; CW, clockwise; DIC, dynamic induction control [Colour figure can be viewed at wileyonlinelibrary.com]

TABLE 3 Turbulent inflow, two-turbine results

	Static 1°	Static 2°	DIC 2.5°	CCW Helix 2.5°	CW Helix 2.5°	DIC 4°	CCW Helix 4°	CW Helix 4°
Power T1 (%)	-1.0	-3.1	-1.1	-1.1	-1.0	-2.8	-2.8	-2.6
Power T2 (%)	+1.6	+5.3	+14.6	+17.2	+6.3	+27.3	+39.5	+18.0
Total power production (%)	-0.3	-1.0	+2.8	+3.4	+0.8	+4.6	+7.5	+2.5
Variance of power T1 (%)	-2.2	-5.8	+79.6	-3.4	-1.4	+194.0	-7.9	-5.1
Variance of power T2 (%)	-11.0	-17.6	+280.8	+143.0	+82.2	+583.6	+239.4	+187.2
Variance of total power (%)	-2.7	-2.9	+121.7	-19.2	+1.1	+342.6	-13.4	-4.4
Variance of thrust T1 (%)	-11.3	-22.1	+580.7	-1.5	+1.1	+1416.7	-3.9	+0.4
Variance of thrust T2 (%)	-13.0	-25.9	+165.1	+71.6	+45.5	+340.9	+123.1	+99.9

Note. All results are relative with respect to the baseline case. Abbreviations: CCW, counterclockwise; CW, clockwise; DIC, dynamic induction control; T1, turbine 1; T2, turbine 2.

4.2 | Two-turbine wind farm

In this section, the performance of a two-turbine wind farm is discussed. The same cases of the single turbine simulations are used, but a second turbine is now placed 5*D* behind the first turbine. In all cases, the second turbine operates at its static optimum, that is, the different control strategies are only implemented on the upstream machine.

The results that are presented here, focus again on the cases with a pitch amplitude of 4°. The power and thrust signals of both turbines in these simulations are shown in Figure 10. As expected, the power production of turbine 2 when DIC is implemented on turbine 1 is slightly higher than with the helix strategies. However, the plot also shows that DIC not only increases the variations in power and thrust of the excited turbine, but also of the downstream turbine. This effect is significantly less pronounced for the helix strategies.

All findings with respect to power and thrust are summarized in Table 3. Notice that the energy increase at 5*D* as predicted in Table 2 corresponds very well with the actual power increase of a turbine at 5*D*. As a result, the CCW helix approach with a 4° pitch amplitude increases the power production of this two-turbine wind farm with 7.5%. This is considerably higher than the 4.6% gain obtained with DIC. The overall energy production of all strategies is shown in Figure 11.

Apart from the power production, it is also interesting to investigate the variations of power and thrust. With both helix approaches, the power and thrust variations of the excited turbine are, in general, slightly reduced. Due to the increased wake velocity and turbulence, the downstream turbines experience a significantly higher power and thrust variations than in the baseline case. However, compared with DIC, these variations are much lower. As a result, the fatigue loads that might lead to structural damage of the wind turbine are expected to be substantially lower than with DIC.

A final note should be made with respect to the performance of the helix approach: as the research presented in this paper serves mainly as a proof of concept, the optimal settings for the helix approach are as of yet unknown. In this study, it was assumed that the optimal excitation

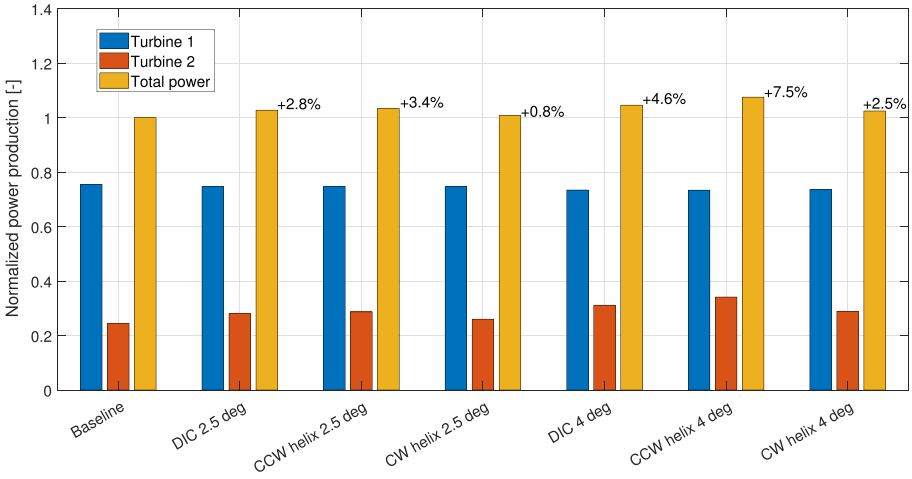

FIGURE 11 Power production of the two-turbine wind farm for the baseline case, dynamic induction control (DIC) and the counterclockwise (CCW) and clockwise (CW) helix. As shown, the power loss at turbine 1 is limited with all methods. The power gain at turbine 2 results in a farm-wide increase in power production with respect to the baseline case [Colour figure can be viewed at wileyonlinelibrary.com]

frequency is identical to the optimal DIC frequency. As such, the 7.5% power gain found here can be considered conservative, as a different dynamic input signal might lead to better performance.

5 | CONCLUSIONS

In this paper, a novel wind farm control strategy is proposed. The strategy involves using IPC to dynamically vary the direction of the thrust force exerted on the flow by a wind turbine, leading to a helical wake that increases mixing. This mixing promotes wake recovery, such that downstream turbines will experience higher wind speeds and subsequently have a higher power production. Due to the helical shape of the wake, this approach is named the helix approach. A proof of concept is given for this novel dynamic wind farm control strategy.

The strategy is tested using high-fidelity LES simulations, proving that the helix approach is effective at increasing wake recovery: the energy in the wake can be increased by up to 47%. Furthermore, it is observed that a helix rotating in CCW direction results in better wake recovery than a helix rotating in CW direction. Finally, these simulations show that the area around the wake exhibits a slightly lower wind speed than in the baseline case. This indicates that the helix approach, similar to DIC, is most effective in the case of full wake interaction between turbines. In the case of partial wake overlap, or when the wind direction is constantly changing, the gains obtained with this approach might diminish. This should therefore be considered a point of attention for future research.

Simulations with a second turbine in the wake of the controlled turbine, located 5 rotor diameters downstream, show that the energy capture can be increased with up to 7.5% for this two-turbine wind farm. As the optimal control settings for the helix approach have not yet been evaluated, this gain should be seen as an indication of its potential, not as an upper limit.

The helix approach is compared with different existing control strategies. The current simulations show that it is a more effective method to increase the energy capture of a wind farm than both static derating and DIC. Compared with the latter, the helix approach results in power and thrust variations that are over a factor 2 lower. Furthermore, compared with DIC or yaw-based wake redirection, the operational strategy used in the helix approach is a less severe deviation from the operating range for which the turbine was designed, assuming the turbines have IPC capabilities. This strategy utilizes the individual pitch capabilities that modern wind turbines possess, but applies a slightly different frequency. This should allow for a much quicker adaptation of the technology by the industry, perhaps delivering a novel wind farm control methodology that can reliably increase the power production in existing wind farms without the need for slow certification protocols and fundamental turbine redesign.

This paper should be considered as a proof of concept. As the helix approach, or dynamic IPC in general, is a completely novel concept, this paper only shows that it *can* be an effective wind farm control strategy. To determine its full potential, further exploration is necessary. Future—potentially crucial—research directions include, but are limited to, studying the difference between the CW and CCW helix, finding the optimal blade excitation signals, investigating the damage equivalent load effects on different components of both the excited and downstream turbine, investigating the effect of the turbulence intensity on the effectiveness of DIPC, applying closed-loop control on the yaw and tilt moments, increasing the farm size to study the effect on turbines further downstream, and executing scaled wind tunnel experiments and full scale tests on an actual wind turbine or wind farm.

CONFLICT OF INTEREST

The authors declare no conflict of interest.

ORCID

Joeri A. Frederik https://orcid.org/0000-0002-4455-2777
Bart M. Doekemeijer https://orcid.org/0000-0003-2757-1615

Sebastiaan P. Mulders https://orcid.org/0000-0003-4689-257X
Jan-Willem van Wingerden https://orcid.org/0000-0003-3061-7442

REFERENCES

1. Jensen NO. A note on wind generator interaction; 1983.
2. Katic I, Højstrup J, Jensen NO. A simple model for cluster efficiency. *European Wind Energy Association Conference and Exhibition*. Rome: A. Raguzzi; 1987:407-410.
3. S Lissaman P. Energy effectiveness of arbitrary arrays of wind turbines. *J Energy*. 1979;3(6):323-328.
4. Annoni J, Fleming P, Scholbrock A, et al. Analysis of control-oriented wake modeling tools using lidar field results. *Wind Energy Sci*. 2018;3(2):819-831.
5. Bastankhah M, Porté-Agel F. Experimental and theoretical study of wind turbine wakes in yawed conditions. *J Fluid Mech*. 2016;806:506-541.
6. Ciri U, Rotea MA, Leonardi S. Model-free control of wind farms: a comparative study between individual and coordinated extremum seeking. *Renew Energy*. 2017;113:1033-1045.
7. Marden JR, Ruben SD, Pao LY. A model-free approach to wind farm control using game theoretic methods. *IEEE Trans Contr Syst Technol*. 2013;21(4):1207-1214.
8. Vali M, van Wingerden J-W, Boersma S, Petrović V, Kühn M. A predictive control framework for optimal energy extraction of wind farms. *Journal of Physics: Conference Series*, Vol. 753. Munich, Germany: IOP Publishing; 2016:52013.
9. Annoni J, Gebraad PM, Scholbrock AK, Fleming PA, van Wingerden J-W. Analysis of axial-induction-based wind plant control using an engineering and a high-order wind plant model. *Wind Energy*. 2016;19(6):1135-1150.
10. Campagnolo F, Petrović V, Bottasso CL, Croce A. Wind tunnel testing of wake control strategies. In: 2016 American Control Conference (ACC). Denver, MA, USA; 2016:513-518.
11. van der Hoek D, Kanev S, Allin J, Bieniek D, Mittelmeier N. Effects of axial induction control on wind farm energy production-a field test. *Renew Energy*. 2019;140:994-1003.
12. Jiménez Á, Crespo A, Migoya E. Application of a LES technique to characterize the wake deflection of a wind turbine in yaw. *Wind Energy*. 2010;13(6):559-572.
13. Howland MF, Bossuyt J, Martínez-Tossas LA, Meyers J, Meneveau C. Wake structure in actuator disk models of wind turbines in yaw under uniform inflow conditions. *J Renew Sustain Energy*. 2016;8(4):43301.
14. Vollmer L, Steinfeld G, Heinemann D, Kühn M. Estimating the wake deflection downstream of a wind turbine in different atmospheric stabilities: An les study. *Wind Energ Sci*. 2016;1:129-141.
15. Fleming P, Gebraad PM, Lee S, et al. Simulation comparison of wake mitigation control strategies for a two-turbine case. *Wind Energy*. 2015;18(12):2135-2143.
16. Gebraad P, Thomas JJ, Ning A, Fleming P, Dykes K. Maximization of the annual energy production of wind power plants by optimization of layout and yaw-based wake control. *Wind Energy*. 2017;20(1):97-107.
17. Raach S, Schlipf D, Cheng PW. Lidar-based wake tracking for closed-loop wind farm control. Munich, Germany; 2016:052009.
18. Campagnolo F, Petrović V, Schreiber J, Nanos EM, Croce A, Bottasso CL. Wind tunnel testing of a closed-loop wake deflection controller for wind farm power maximization. *J Phys Conf Ser*. 2016;753(3):7.
19. Fleming P, Annoni J, Shah JJ, et al. Field test of wake steering at an offshore wind farm. *Wind Energy Sci*. 2017;2(1):229-239.
20. Howland MF, Lele SK, Dabiri JO. Wind farm power optimization through wake steering. *Proc National Acad Sci*. 2019;116(29):14495-14500.
21. Energy SGR. Siemens gamesa now able to actively dictate wind flow at offshore wind locations. https://www.siemensgamesa.com/en-int/newsroom/2019/11/191126-siemens-gamesa-wake-adapt-en; 2019.
22. Boersma S, Doekemeijer B, Gebraad PM, et al. A tutorial on control-oriented modeling and control of wind farms. In: 2017 American Control Conference (ACC) . Seattle, WA, USA: IEEE; 2017:1-18.
23. Kheirabadi AC, Nagamune R. A quantitative review of wind farm control with the objective of wind farm power maximization. *J Wind Eng Indust Aerodyn*. 2019;192:45-73.
24. Westergaard CH. A method for improving large array wind park power performance through active wake manipulation reducing shadow effects; 2013.
25. Goit JP, Meyers J. Optimal control of energy extraction in wind-farm boundary layers. *J Fluid Mech*. 2015;768:5-50.
26. Munters W, Meyers J. Effect of wind turbine response time on optimal dynamic induction control of wind farms. *Journal of Physics: Conference Series*, Vol. 753. Munich, Germany: IOP Publishing; 2016:52007.
27. Munters W, Meyers J. An optimal control framework for dynamic induction control of wind farms and their interaction with the atmospheric boundary layer. *Phil Trans R Soc A*. 2017;375(2091):20160100.
28. Munters W, Meyers J. Towards practical dynamic induction control of wind farms: analysis of optimally controlled wind-farm boundary layers and sinusoidal induction control of first-row turbines. *Wind Energy Sci*. 2018;3(1):409-425.
29. Frederik JA, Campagnolo F, Cacciola S, et al. Periodic dynamic induction control of wind farms: proving the potential in simulations and wind tunnel experiments. *Wind Energy Sci*. 2019;5:245–257. under review.
30. Kimura K, Tanabe Y, Matsuo Y, Iida M. Forced wake meandering for rapid recovery of velocity deficits in a wind turbine wake. In: AIAA Scitech 2019 Forum. San Diego, CA, USA; 2019:2083.
31. Munters W, Meyers J. Dynamic strategies for yaw and induction control of wind farms based on large-eddy simulation and optimization. *Energies*. 2018;11(1):177.
32. Bossanyi EA. Individual blade pitch control for load reduction. *Wind Energy: Int J Prog Appl Wind Power Conv Technol*. 2003;6(2):119-128.
33. Bossanyi EA. Further load reductions with individual pitch control. *Wind Energy: Int J Prog Appl Wind Power Conv Technol*. 2005;8(4):481-485.

34. Mulders SP, Pamososuryo AK, Disario GE, van Wingerden JW. Analysis and optimal individual pitch control decoupling by inclusion of an azimuth offset in the multiblade coordinate transformation. *Wind Energy*. 2019;22(3):341-359.
35. Frederik JA, Kröger L, Gülker G, van Wingerden J-W. Data-driven repetitive control: wind tunnel experiments under turbulent conditions. *Contr Eng Pract*. 2018;80:105-115.
36. Frederik JA, Kröger L, Peinke J, Hölling M, van Wingerden J-W. Validating subspace predictive repetitive control under turbulent wind conditions with wind tunnel experiment. *Journal of Physics: Conference Series*, Vol. 1037. Milan, Italy: IOP Publishing; 2018:32008.
37. Navalkar ST, van Wingerden J-W, van Solingen E, Oomen T, Pasterkamp E, Van Kuik G. Subspace predictive repetitive control to mitigate periodic loads on large scale wind turbines. *Mechatronics*. 2014;24(8):916-925.
38. Fleming PA, Gebraad PM, Lee S, et al. Evaluating techniques for redirecting turbine wakes using SOWFA. *Renew Energy*. 2014;70:211-218.
39. van Wingerden JW, Frederik JA, Doekemeijer BM. Enhanced wind turbine wake mixing; 2019.
40. Churchfield M, Lee S. NWTC design codes-SOWFA, 15013 Denver West Parkway, Golden, CO, National Renewable Energy Laboratory (NREL); 2012. http://wind.nrel.gov/designcodes/simulators/SOWFA
41. Churchfield MJ, Lee S, Michalakes J, Moriarty PJ. A numerical study of the effects of atmospheric and wake turbulence on wind turbine dynamics. *J Turbul*. 2012;13:N14.
42. Sørensen JN, Shen WZ. Numerical modeling of wind turbine wakes. *J Fluids Eng*. 2002;124(2):393-399.
43. Bak C, Zhale F, Bitsche R, et al. The dtu 10-MW reference wind turbine. Kongens Lyngby, Denmark: Technical University of Denmark (DTU), Department of Wind Energy; 2013. http://dtu-10mw-rwt.vindenergi.dtu.dk/
44. Nilsson K, Ivanell S, Hansen KS, et al. Large-eddy simulations of the Lillgrund Wind Farm. *Wind Energy*. 2015;18(3):449-467.
45. Bir G. Multi-blade coordinate transformation and its application to wind turbine analysis. In: 46th AIAA Aerospace Sciences Meeting and Exhibit. Reno, NV, USA; 2008:1300.

How to cite this article: Frederik JA, Doekemeijer BM, Mulders SP, van Wingerden J-W. The helix approach: using dynamic individual pitch control to enhance wake mixing in wind farms. *Wind Energy*. 2020;23:1739–1751. https://doi.org/10.1002/we.2513